Inorganic Chemistry

Article

pubs.acs.org/IC

Interaction between the Heme and a G-Quartet in a Heme−DNA Complex

Kaori Saito,[†] Hulin Tai,[†] Hikaru Hemmi,[‡] Nagao Kobayashi,*[,§] and Yasuhiko Yamamoto*[,†]

[†]Department of Chemistry, University of Tsukuba, Tsukuba 305-8571, Japan

[‡]National Food Research Institute, National Agriculture and Food Research Organization, Tsukuba 305-8642, Japan

[§]Department of Chemistry, Graduate School of Science, Tohoku University, Sendai 980-8578, Japan

Supporting Information

ABSTRACT: The structure of a complex between heme(Fe^{3+}) and a parallel G-quadruplex DNA formed from a single repeat sequence of the human telomere, d(TTAGGG), has been characterized by ^1H NMR. The study demonstrated that the heme(Fe^{3+}) is sandwiched between the 3′-terminal G-quartets of the G-quadruplex DNA. Hence, the net +1 charge of the heme(Fe^{3+}) in the complex is surrounded by the eight carbonyl oxygen atoms of the G-quartets. Interaction between the heme Fe^{3+} and G-quartets in the complex was clearly manifested in the solvent $^1H/^2H$ isotope effect on the NMR parameters of paramagnetically shifted heme methyl proton signals, and interaction of the heme Fe^{3+} with the eight carbonyl oxygen atoms of the two G-quartets was shown to provide a strong and axially symmetric ligand field surrounding the heme Fe^{3+}, yielding a heme(Fe^{3+}) low-spin species with a highly symmetric heme electronic structure. This finding provides new insights as to the design of the molecular architecture and functional properties of various heme−DNA complexes.

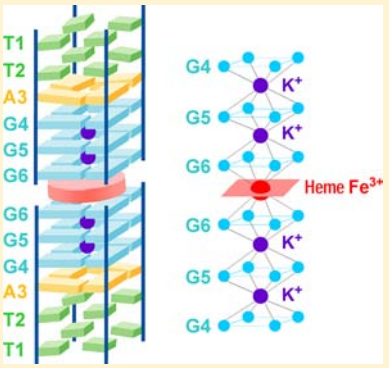

INTRODUCTION

A G-quadruplex DNA is composed of stacked G-quartets (see inset of Figure 1), each of which involves the planar association of four guanine bases circularly connected through Hoogsteen-type base-pairings.[1−4] The size and planarity of a G-quartet are well-suited for interaction with a porphyrin ring through $\pi-\pi$ stacking. The complexation of G-quadruplex DNAs with porphyrin or metal−porphyrin derivatives has been studied extensively to characterize their molecular recognition of each other[5−14] as well as to create catalytic DNAs that exhibit various functions.[15−20]

In the presence of an appropriate K^+ concentration, a single repeat sequence of the human telomere, d(TTAGGG), forms all-parallel G-quadruplex DNA,[21] which further assembles into a "dimer" through end-to-end stacking of the 3′-terminal G-quartets.[22] We have demonstrated that heme with either ferric or ferrous iron, that is, the iron(III)− or iron(II)−protoporphyrin IX complex [heme(Fe^{3+}) or heme(Fe^{2+}), respectively] (see inset of Figure 1), binds to G-quadruplex DNA formed from d(TTAGGG) to form a stable "heme−DNA complex", which exhibits spectroscopic and functional properties remarkably similar to those of hemoproteins.[9,12−14] For example, as in the cases of various hemoproteins,[23−28] heme(Fe^{3+}) in the complex exhibits a characteristic pH-dependent spin equilibrium between the high-spin (HS) state, $S = {}^5/_2$, and the low-spin (LS) state, $S = {}^1/_2$, at low and high pH, respectively, with a midpoint at pH = 8.6 ± 0.3.[9] Furthermore, carbon monoxide (CO) can also be bound to the heme(Fe^{2+})−DNA complex, yielding a CO adduct, and heme Fe^{2+} bound to CO as an axial ligand adopts an LS configuration with $S = 0$.[13] We have carried out NMR structural characterization of the CO adduct of the complex and revealed that heme(Fe^{2+}) binds to the 3′-terminal G-quartets of the DNA though $\pi-\pi$ stacking interactions between the porphyrin moiety of the heme and the G-quartets.[14] The $\pi-\pi$ stacking interaction between the pseudo-C_2-symmetric heme and the C_4-symmetric G-quartet in the complex resulted in the formation of two isomers possessing heme orientations differing by 180° rotation about the pseudo-C_2-axis with respect to the DNA, and as has been demonstrated for various *b*-type hemoproteins,[29−33] these two slowly interconverting heme orientational isomers were formed in a ratio of ∼1:1. Furthermore, electrostatic interaction between heme Fe^{2+} and the four carbonyl oxygen atoms of a 3′-terminal G-quartet is also likely to contribute to the stability of the complex, as was proposed previously.[34] Such electrostatic interaction is expected to be stronger in a heme(Fe^{3+})−DNA complex due to the net +1 charge of the heme.

In this study, the structure of the LS form of the heme(Fe^{3+})−DNA complex has been investigated in order to characterize the interaction between heme(Fe^{3+}) and the 3′-terminal G-quartets in the complex. The study demonstrated that heme(Fe^{3+}) is sandwiched between the 3′-terminal G-quartets of the G-quadruplex DNA. As a result, the net +1 charge of the heme(Fe^{3+}) in the complex is surrounded by the eight carbonyl oxygen atoms of the G-quartets. In fact, the interaction between the heme Fe^{3+} and G-quartets in the

Received: March 19, 2012
Published: July 25, 2012

   dx.doi.org/10.1021/ic3005739 | *Inorg. Chem.* 2012, 51, 8168−8176

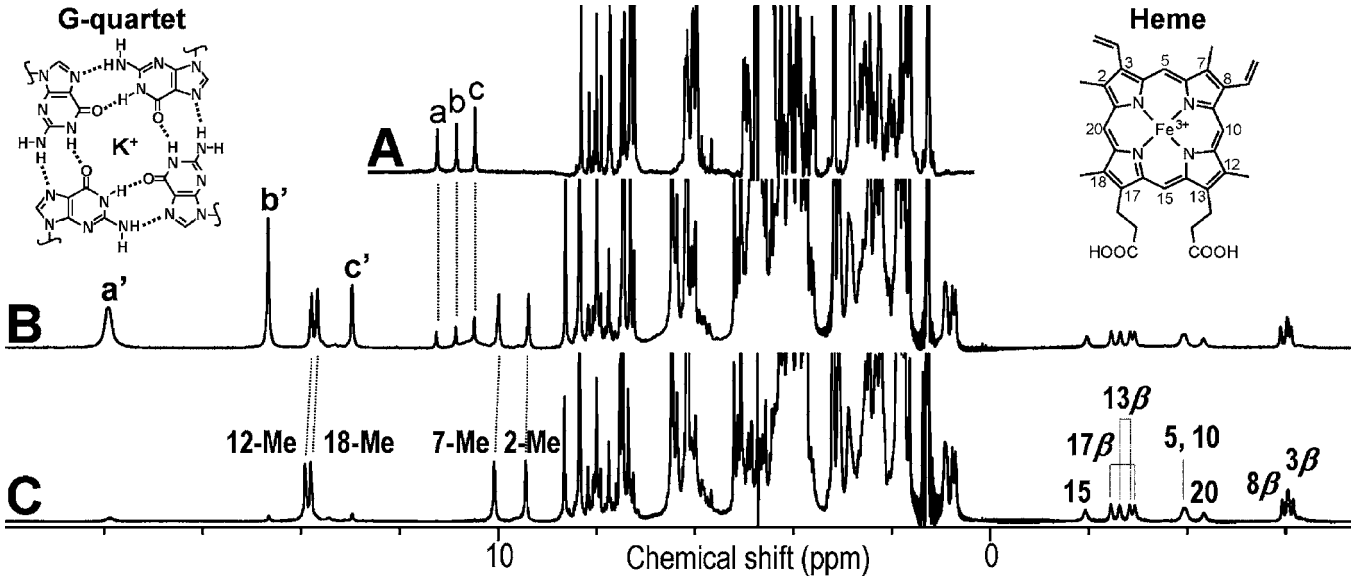

Figure 1. The 600 MHz ^{1}H NMR spectra of G-quadruplex DNA, d[(TTAGGG)]$_4$ (A) in the absence and (B, C) in the presence of 0.5 equiv of heme(Fe^{3+}) in (A, B) 90% ^1H_2O/10% ^2H_2O or (C) 2% ^1H_2O/98% ^2H_2O, with 300 mM KCl and 50 mM potassium phosphate buffer at pH 9.80 and 25 °C. The molecular structure of the G-quartet is schematically illustrated in the upper left corner, and that of heme(Fe^{3+}) is shown in the upper right corner. Peaks a–c and a′–c′ are due to guanine imino protons of the free and heme(Fe^{3+})-bound DNAs, respectively. Signal assignments of heme side chain protons are given in trace C. The small differences in shift between the corresponding signals in traces B and C are due to a solvent ^{1}H/^{2}H isotope effect.

complex was clearly manifested in the solvent ^{1}H/^{2}H isotope effect on the NMR parameters of paramagnetically shifted heme proton signals. The interaction between heme Fe^{3+} and the carbonyl oxygen atoms of the G-quartets in the complex was found to be strong enough to yield a stable LS form. These results suggested the formation of novel coordination bonds between the heme Fe^{3+} and the G-quartets. This study may pave the way to a new research field of coordination chemistry of the heme–DNA complex.

MATERIALS AND METHODS

Sample Preparation. d(TTAGGG) purified with a C-18 Sep-Pak cartridge was purchased from Tsukuba Oligo Service Co. The oligonucleotide was obtained by ethanol precipitation and then desalted with a Microcon YM-3 membrane (Millipore, Bedford, MA). The concentration of the oligonucleotide was determined spectrophotometrically via the absorbance at 260 nm (molar extinction coefficient $\varepsilon_{260} = 6.89 \times 10^4$ cm^{-1}·M^{-1}). Heme(Fe^{3+}) was purchased from Sigma–Aldrich Co. Preparation of the heme(Fe^{3+})–DNA complex was carried out as described previously.[14] For NMR sample preparation of the heme–DNA complex, 270 μL of 2.2 mM DNA, as a quadruplex form, in 333.3 mM KCl and 55.6 mM potassium phosphate buffer, pH 7.0, was mixed with 30 μL of 10 mM heme dissolved in 50 mM KOH, and then the pH of the resulting solution was adjusted to 9.80 with 0.2 M KOH, if necessary. Thus, the final concentrations of both DNA and heme in the solution mixture were 2 mM. The ^2H_2O content of the samples was either ∼10% or ∼98%.

NMR Measurements. ^{1}H NMR spectra were recorded on Bruker Avance-600 and Avance-500 spectrometers operating at ^{1}H frequencies of 600 and 500 MHz, respectively. One-dimensional ^{1}H NMR spectra of the heme–DNA complex were obtained with a 35 ppm spectral width, 32K data points, a 1.5 s relaxation delay, and 512 transients. Water suppression was achieved by the watergate or presaturation method.[35,36] The signal-to-noise ratio of the spectra was improved by apodization, which introduced 0.3 Hz line-broadening. The NMR spectra were processed by use of XWIN-NMR version 3.5 (Bruker BioSpin), and intensity analysis of the signals was performed with MestRe-c version 4.8.6.0 (Mestrelab Research). Two-dimensional nuclear Overhauser effect (NOESY) spectra of the heme–DNA complex were acquired by quadrature detection in the phase-sensitive mode with a States time-proportional phase incrementation (TPPI),[37] with a 30 ppm spectral width, 4K × 512 data points, a 1.5 s relaxation delay, and a mixing time of 150 ms at 25 °C. A phase-shifted sine-squared window function was applied to both dimensions before two-dimensional Fourier transformation. The chemical shifts for ^{1}H NMR spectra are referred to external 2,2-dimethyl-2-silapentane-5-sulfonate.

Absorption, Circular Dichroism, and Magnetic Circular Dichroism Measurements. Absorption spectra were recorded on a Beckman DU640 spectrometer over the spectral range 305–495 nm. In order to characterize the complexation between heme(Fe^{3+}) and [d(TTAGGG)]$_4$, 4.0 μM heme(Fe^{3+}) in 300 mM KCl and 50 mM potassium carbonate buffer, pH 10.10, together with 0.08% (w/v) Triton X-100 and 0.5% (v/v) dimethyl sulfoxide (DMSO) to prevent heme aggregation, was titrated against the DNA at 25 °C. Circular dichroism (CD) and magnetic circular dichroism (MCD) spectra were recorded on a Jasco J-725 spectrodichrometer equipped with a Jasco electromagnet, which produces magnetic fields of up to 1.09 T with both parallel and antiparalle1 fields. The CD and MCD magnitudes were expressed in terms of molar ellipticity ($[\theta]$ in deg·dm^{-3}·mol^{-1}·cm^{-1}) and molar ellipticity per tesla ($[\theta]_M$ in deg·dm^{-3}·mol^{-1}·cm^{-1}·T^{-1}), respectively.

RESULTS

^{1}H NMR Spectra of [d(TTAGGG)]$_4$ and the Heme–DNA Complex. We first characterized the assembly of d(TTAGGG) at pH 9.80 and 25 °C by ^{1}H NMR. In the 600 MHz ^{1}H NMR

dx.doi.org/10.1021/ic3005739 | Inorg. Chem. 2012, 51, 8168–8176

spectrum of the DNA (Figure 1A), three signals, a–c, due to the G4, G5, and G6 imino protons, respectively, were observed in the chemical shift region characteristic of a G-quartet, >10 ppm,[21] confirming not only the formation of an all-parallel G-quadruplex DNA but also the C_4 symmetry of its structure. In addition, the nuclear Overhauser effect (NOE) connectivities observed at pH 9.80 were essentially identical to those at pH 7.00,[11] although some signals exhibited pH-dependent shift changes of <0.03 ppm (see Table S1 in the Supporting Information). These results indicated that the formation and structure of a G-quadruplex DNA formed from d(TTAGGG) are independent of pH up to at least 9.80. The all-parallel G-quadruplex DNA assembled from this sequence has been shown to dimerize through end-to-end stacking of the 3′-terminal G-quartets in the presence of a high K^+ concentration,[22] and under the conditions used in the study, the DNA exists predominantly as the dimer, as judged from the shifts of the G4, G5, and G6 imino protons[22] (Figure 1A and Table S1 in the Supporting Information).

We then added 0.50 equiv of heme(Fe^{3+}) to the DNA to prepare a heme(Fe^{3+})–DNA complex. Upon heme(Fe^{3+}) addition, many signals newly appeared in the spectrum (Figure 1B). When the solvent was changed to ^2H_2O, newly appearing signals a′–c′, in addition to signals a–c, vanished almost completely (Figure 1C). Exchangeable proton signals a′–c′ were assigned to the imino protons of G6, G5, and G4, respectively, on the basis of observed intramolecular NOEs (Figure 2). Consequently, the G4, G5, and G6 imino proton signals were found to exhibit heme(Fe^{3+})-induced shift changes ($\Delta\delta_{heme}$) of +1.73, +3.83, and +7.47 ppm, respectively (Figure 1 and Table 1). The largest $\Delta\delta_{heme}$ value observed for the G6 imino proton signal clearly indicated that heme(Fe^{3+}) stacks onto the G6 G-quartets in the complex. The $\Delta\delta_{heme}$ value could be interpreted mainly in terms of the shift induced by the ring current of the porphyrin moiety of heme (δ_{ring})[14] and the paramagnetic shift due to an unpaired electron of heme Fe^{3+} (δ_{para}), the δ_{ring} and δ_{para} contributions to the $\Delta\delta_{heme}$ value being negative and positive, respectively. Consequently, observation of positive $\Delta\delta_{heme}$ values for these imino proton signals indicated that the δ_{para} value is more important than the δ_{ring} one for determination of $\Delta\delta_{heme}$.

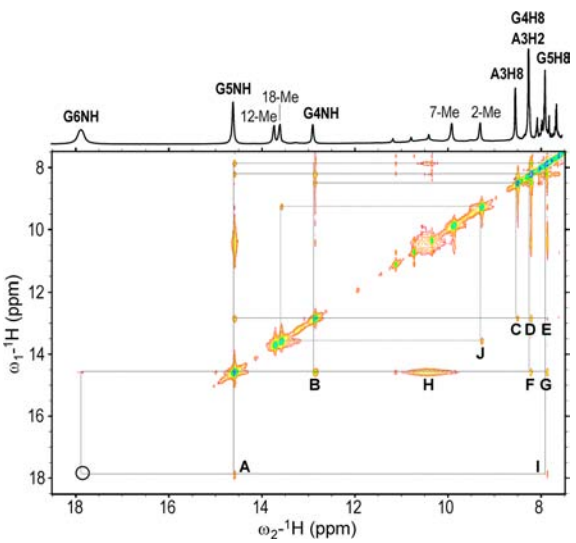

Figure 2. A portion of the NOESY spectrum of $[d(TTAGGG)]_4$ in the presence of 0.5 equiv of heme(Fe^{3+}) in 90% ^1H_2O/10% ^2H_2O, 300 mM KCl, and 50 mM potassium phosphate buffer at pH 9.80 and 25 °C. A mixing time of 150 ms was used to record the spectrum. Signal assignments of selected proton signals are shown with the spectrum. Due to considerable line broadening, a diagonal peak for a G6 imino proton (G6NH) was not seen in the spectrum but could be observed at the position indicated by a circle with a lower contour level. Cross peaks A–J indicate the connectivities of the following proton pairs: (A) G6NH–G5NH, (B) G5NH–G4NH, (C) G4NH–A3H8, (D) G4NH–A3H2 and G4NH–G4H8, (E) G4NH–G5H8, (F) G5NH–G4H8, (G) G5NH–G5H8, (H) G5NH–G5NH2, (I) G6NH–G5H8, and (J) heme 18-Me–heme 2-Me.

The interaction between heme(Fe^{3+}) and 3′-terminal (G6) G-quartets in the complex could be confirmed by the observation of intermolecular NOEs between the heme (methyl and vinyl) and G6 (H8 and H1′–H4′) proton signals (Figure 3, and Figures S1 and S2 in the Supporting Information). Furthermore, the shift difference between the G4 imino proton signals of the free and heme(Fe^{3+})-bound DNAs, 1.73 ppm, indicated that the time scale of the heme(Fe^{3+}) binding to the DNA is $\ll 10^2$ s^{-1}. The observed NOEs also allowed assignment of most DNA proton signals of the complex and all the heme proton ones (Tables 1 and 2, and Figures S3 and S4 in the Supporting Information). In contrast to the CO adduct of the heme(Fe^{2+})–DNA complex, which exhibited two sets of heme proton signals due to the presence of heme orientational isomers,[14] only a single set of heme proton signals was observed in the spectra of the present complex, indicating the absence of heme orientational isomers. On the other hand, in the 600 MHz ^1H NMR spectra of the present complex, G6 ribose H1′, H2′, H2″, and H4′ proton signals appeared as ~1:1 doublet peaks with splitting of 0.02–0.07 ppm (Table 1, Figure 3, and Figures S5 and S6 in the Supporting Information), indicating that 4-fold (8-fold if the DNA dimer is considered as a unit) degeneracy of these protons is removed upon heme(Fe^{3+}) binding to the DNA. These protons are expected to be located in close proximity to heme(Fe^{3+}) in the complex, and hence their shifts are likely to be subject to the effect of unpaired electron of the heme(Fe^{3+}). Consequently, the ~1:1 splitting of these proton signals could be attributed to the rhombic component of the magnetic susceptibility tensor due to the unpaired electron, which is 2-fold symmetric with respect to the heme normal.[38]

Finally, we examined the ^1H NMR spectra of the heme(Fe^{3+})–DNA complex at various temperatures (Figure 4). At high temperatures, thermal denaturation of the DNA resulted in disappearance of the imino proton signals. As shown in Figure 4, the intensity ratio of the imino proton signals of the free DNA to those of the heme(Fe^{3+})-bound DNA decreased with increasing temperature, clearly demonstrating that the thermostability of the DNA is enhanced by heme(Fe^{3+}) binding.

Solvent $^1H/^2H$ Isotope Effects on NMR Spectral Parameters of Heme(Fe^{3+}) Bound to DNA. The downfield-shifted portions of the ^1H NMR spectra of the heme(Fe^{3+})-DNA complex with various ^2H_2O contents are compared in Figure 5. In addition to disappearance of the G4–G6 imino proton signals of both the free and heme(Fe^{3+})-bound DNAs with increasing ^2H_2O content of the solvent, two features are noticeable as to the effect of the solvent $^1H/^2H$ isotope on heme methyl proton signals. One is the progressive downfield shifts with increasing ^2H_2O content: the heme 12-, 18-, 7-, and 2-Me signals observed with ^2H_2O content of ~98% were downfield-shifted relative to the corresponding signals

dx.doi.org/10.1021/ic3005739 | Inorg. Chem. 2012, 51, 8168–8176

Table 1. Chemical Shifts and Heme-Induced Shift Changes of the Heme(Fe^{3+})−$[d(TTAGGG)]_4$ Complex[a]

	Chemical Shift (ppm)													
	H1′		H2′/H2″		H3′		H4′		H5′/H5″		H6/H8		NH/Me/H2	
	free	complex	free	complex	free	complex	free	complex	free	complex	free	complex	free	complex
T1	5.95	6.02	2.03, 2.27	2.08, 2.31	4.58		3.94	3.96	3.57, 3.62	3.59, 3.63	7.31	7.33	1.62	1.64
T2	6.15	6.24	1.97, 2.25	2.07, 2.36	4.66	4.71	4.00	4.06		3.88, 3.89	7.22	7.31	1.70	1.77
A3	6.19	6.34	2.82	2.94	5.01	5.07	4.39	4.43	4.03, 4.09	4.08, 4.12	8.31	8.51	7.99	8.22
G4	5.96	6.24	2.52, 2.83	2.76, 2.96	4.92	4.93	4.45	4.23		2.76, 2.96	7.72	8.22	11.23	12.96
G5	6.04	6.03	2.64, 2.82		4.98		4.42	4.31			7.43	7.87	10.84	14.67
G6	6.05	4.91/4.98	2.55, 2.78	0.55/0.61, 0.74/0.77	4.80	3.72	4.26	2.18/2.20			7.28	6.31	10.46	17.93

	$\Delta\delta_{heme}$[b] (ppm)						
	H1′	H2′/H2″	H3′	H4′	H5′/H5″	H6/H8	NH/Me/H2
T1	0.07	0.05, 0.04		0.02	0.02, 0.01	0.02	0.02
T2	0.09	0.10, 0.11	0.05	0.06		0.09	0.07
A3	0.15	0.12	0.06	0.04	0.05, 0.03	0.20	0.23
G4	0.28	0.24, 0.13	0.01	−0.22		0.50	1.73
G5	−0.01			−0.11		0.44	3.83
G6	−1.14/−1.07	−2.00/−1.94, −2.04/−2.01	−1.08	−2.08/−2.01		−0.98	7.47

[a] In 90% ^1H_2O/10% ^2H_2O, 300 mM KCl, and 50 mM potassium phosphate buffer at pH 9.80 and 25 °C. [b] $\Delta\delta_{heme} = \delta_{complex} - \delta_{free}$.

with ^2H_2O content of ∼10% by 0.13, 0.12, 0.10, and 0.06 ppm, respectively. The other is that the line widths of the heme methyl proton signals of the heme(Fe^{3+})−DNA complex were affected by the ^2H_2O content, being largest with ^2H_2O contents of ∼50%. Since the heme propionic acid side chains should be deprotonated at the pH value used in this study, no exchangeable proton is associated with the heme(Fe^{3+}) in the complex. Consequently, these subtle but significant solvent $^1H/^2H$ isotope effects on the NMR spectral parameters of the heme methyl proton signals should be due to the effect of solvent $^1H/^2H$ isotope exchange of DNA protons, most likely G6 imino protons, on the heme electronic structure in the complex (see below).

Selective Spin−Lattice Relaxation Times of Imino Protons of the Free and Heme(Fe^{3+})-Bound DNAs. We also measured the selective spin−lattice relaxation times (T_1^{sel}) of the imino protons of the free and heme(Fe^{3+})-bound DNAs in order to estimate the orientation of these protons relative to heme Fe^{3+} in the heme(Fe^{3+})−DNA complex. The T_1^{sel} values of the G4, G5, and G6 imino protons of the free DNA were determined to be 270 ± 30, 510 ± 50, and 510 ± 50 ms, respectively (Figure S7 in the Supporting Information), and were shortened by factors of ∼1/1.2, ∼1/3.2, and ∼1/26, respectively, upon heme(Fe^{3+}) binding; that is, T_1^{sel} values of 230 ± 50, 160 ± 30, and 20 ± 10 ms were obtained for the G4, G5, and G6 imino protons of the heme(Fe^{3+})−DNA complex, respectively (Figures S8 in the Supporting Information). The shorter T_1^{sel} value for the G4 imino proton of the free DNA, compared with those for G5 and G6, could be due to its faster hydrogen exchange reaction with the solvent, because the G4 proton is more exposed to the solvent compared with the other two in the DNA dimer. The remarkable shortening of the T_1^{sel} value for the G6 imino proton indicated that relaxation of the G6 imino proton is significantly affected by paramagnetic relaxation due to an unpaired electron of heme Fe^{3+}, indicating that, among the three imino protons, the G6 one is located most closely to heme Fe^{3+} in the heme(Fe^{3+})−DNA complex. This result is consistent with the interaction between the heme(Fe^{3+}) and G6 G-quartets in the complex.

Determination of Stoichiometry and Binding Constant of the Heme(Fe^{3+})−DNA Complex. The slow hydrogen exchange reaction of the imino protons of both the free and heme(Fe^{3+})-bound DNAs, as manifested in the well-resolved signals for these protons (Figure 1B), and the slow heme(Fe^{3+}) binding reaction, that is, a time scale of $\ll 10^2$ s^{-1} (see above), allowed quantitative analysis of the NMR signal intensities. A stoichiometric ratio of 1:2 for heme(Fe^{3+}):G-quadruplex DNA in the complex was determined through analysis of the intensities of signals due to DNA imino and heme methyl protons (Figure 1B and Figure S9 in the Supporting Information).

The absorption spectra of heme(Fe^{3+}) at pH 10.10 in the presence of various stoichiometric ratios of the G-quadruplex DNA formed from d(TTAGGG) showed that, upon addition of the DNA, the Soret band due to the porphyrin π system of heme(Fe^{3+}) exhibited a red shift from 390 to 406 nm associated with ∼140% hyperchromism, and isosbestic points were observed at 389, 425, and 480 nm (see Figure S10 in the Supporting Information). The observation of these isosbestic points shows the occurrence of equilibrium between two distinctly different environments for the porphyrin moiety of heme(Fe^{3+}) in the solution mixture. Scatchard plots of the 406-nm absorption could be satisfactorily represented as a straight line, yielding values of (9 ± 5) × 10^6 M^{-1} and 0.5 ± 0.1 for the association constant (K_a) and total number of binding sites, respectively (see Figure S10 in the Supporting Information). These optical results indicated that heme(Fe^{3+}) and the DNA form a stable 1:2 complex [that is, 1:1 complexation occurs between heme(Fe^{3+}) and the DNA dimer] and hence were consistent with those of the NMR study.

Magnetic Circular Dichroism and Circular Dichroism Spectra of the Heme(Fe^{3+})−DNA Complex. We finally measured magnetic circular dichroism (MCD) and circular dichroism (CD) spectra of the heme(Fe^{3+})−DNA complex at pH 9.80 in order to characterize the axial ligands of the heme Fe^{3+}. The intense *A*-term Soret MCD at ∼410 nm and the very weak negative MCD trough at 610−650 nm (porphyrin-to-iron charge transfer)[39,40] were consistent with a heme(Fe^{3+}) LS species (Figure 6).[41−44] Indeed, the intensity ratio of Soret

dx.doi.org/10.1021/ic3005739 | Inorg. Chem. 2012, 51, 8168−8176

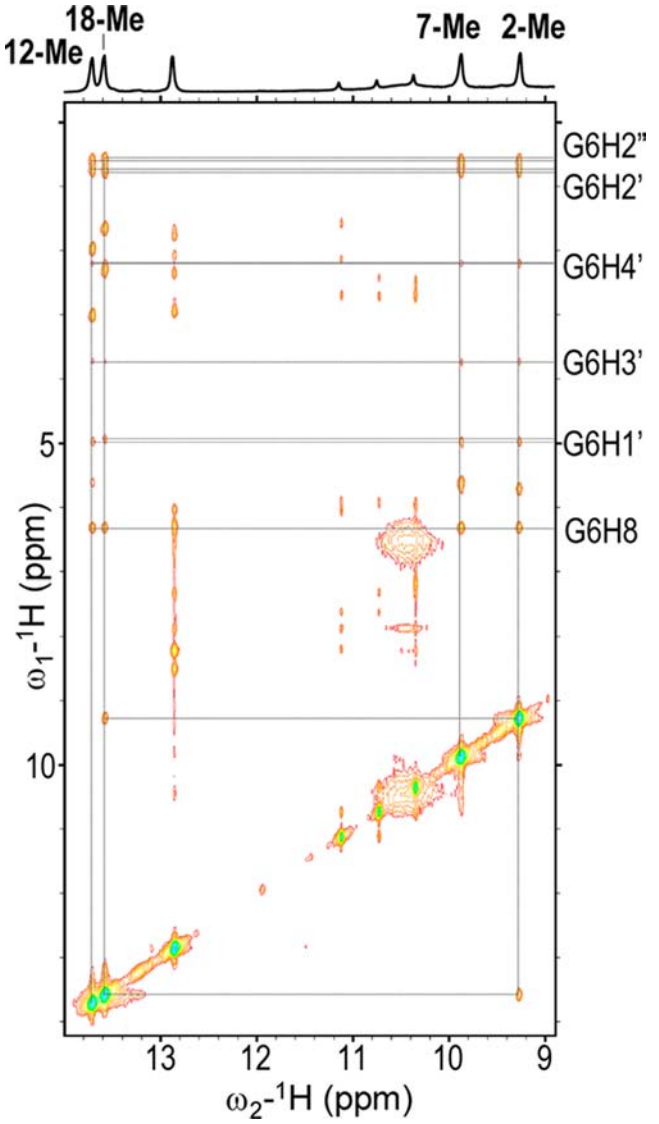

Figure 3. A portion of the NOESY spectrum of $[d(TTAGGG)]_4$ in the presence of 0.5 equiv of heme(Fe^{3+}) in 90% ^1H_2O/10% ^2H_2O, 300 mM KCl, and 50 mM potassium phosphate buffer at pH 9.80 and 25 °C. A mixing time of 150 ms was used to record the spectrum. Signal assignments of four heme methyl and selected G6 proton signals are shown with the spectrum. Intermolecular NOE connectivities between heme and G6 proton signals are indicated by broken lines.

MCD to Q MCD (Figure 6, left) is very close to that of the alkaline form (LS species) of ferric horseradish peroxidase,[43] and the spectroscopic shape in the visible region (Figure 6, right) is similar to that of ferric myoglobin (Mb) with two axial imidazole ligands, which can be classified as a typical LS species.[44] In addition, the negative CD in the Soret and Q regions of the heme(Fe^{3+})–DNA complex (Figure 6), as opposed to the mostly positive CD in the corresponding regions of ferric Mb (see Figures S11–S14 in the Supporting Information), suggested that the axial ligands are located in close proximity to the heme π-system and indicated that the heme(Fe^{3+}) in the complex is surrounded by a right-handed helical environment,[45,46] as a result of an interaction between the heme(Fe^{3+}) and a G-quartet.

Table 2. Chemical Shifts of Heme ^1H NMR Signals of the Heme(Fe^{3+})–$[d(TTAGGG)]_4$ Complex[a]

heme proton	chemical shift (ppm)
Methyls	
2-Me	9.27
7-Me	9.87
12-Me	13.71
18-Me	13.58
Vinyls	
3α	5.71
8α	5.60
8β	−6.14, −6.28
3β	−6.25, −6.35
Meso	
5	−4.24
10	−4.26
15	−2.28
20	−4.62
Propionic	
13α-CH_2	−2.82, −3.02
17α-CH_2	−2.64, −3.11
13β-CH_2	3.00, 1.97
17β-CH_2	2.30, 1.67

[a]In 90% ^1H_2O/10% ^2H_2O, 300 mM KCl, and 50 mM potassium phosphate buffer at pH 9.80 and 25 °C.

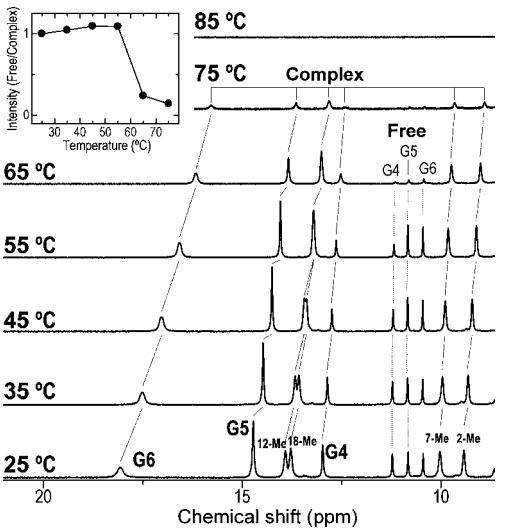

Figure 4. Downfield-shifted portions of the 500 MHz ^1H NMR spectra of $[d(TTAGGG)]_4$ in the presence of 0.3 equiv of heme(Fe^{3+}) in 90% ^1H_2O/10% ^2H_2O, 300 mM KCl, and 50 mM potassium phosphate buffer at pH 9.80 and the indicated temperatures. Plots of the normalized ratio of the total intensity of the imino proton signals, $\Sigma_i I(i)$, where $I(i)$ represents the signal intensity of i (i = imino proton of G4, G5, or G6), of the free DNA to that of the heme(Fe^{3+})-bound DNA [intensity (free/complex)] against temperature are illustrated in the inset. The intensity (free/complex) value was normalized in such a way that the value at 25 °C equaled 1.0. The plots exhibited a sharp decrease above 55 °C, demonstrating that the thermostability of the DNA is enhanced by heme(Fe^{3+}) binding.

DISCUSSION

Structure of the Heme(Fe^{3+})–DNA Complex. The $\Delta\delta_{heme}$ (Table 1) and T_1^{sel} values obtained for the imino proton signals suggested that heme(Fe^{3+}) stacks onto the G6 G-quartets of $[d(TTAGGG)]_4$ in the complex under the

dx.doi.org/10.1021/ic3005739 | Inorg. Chem. 2012, 51, 8168–8176

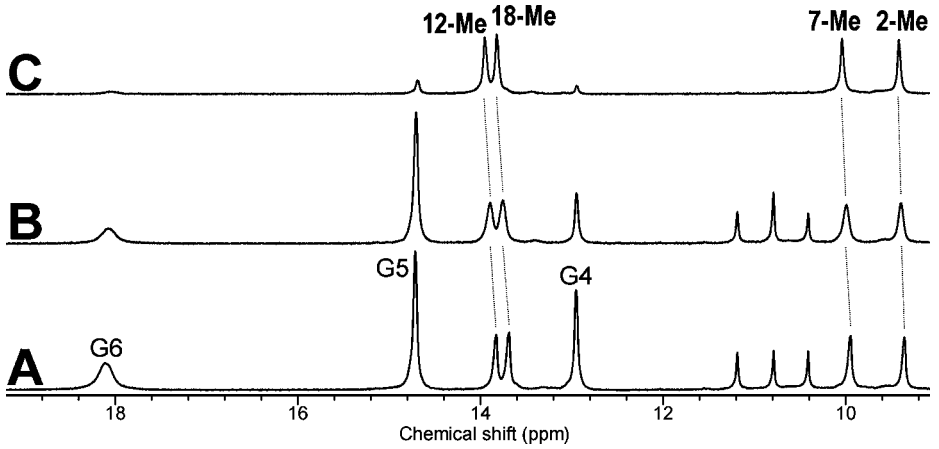

Figure 5. Downfield-shifted portions of the 600 MHz ^{1}H NMR spectra of $[d(TTAGGG)]_4$ in the presence of 0.3 equiv of heme(Fe^{3+}) in (A) 90% ^1H_2O/10% ^2H_2O, (B) 50% ^1H_2O/50% ^2H_2O, and (C) 2% ^1H_2O/98% ^2H_2O with 300 mM KCl and 50 mM potassium phosphate buffer at pH 9.80 and 25 °C. The shifts and line widths of all four heme side-chain methyl proton signals were affected by the ^2H_2O content.

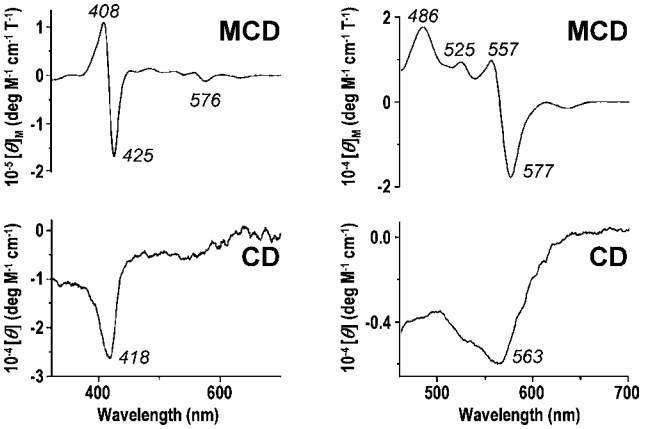

Figure 6. MCD (top) and CD (bottom) spectra of $[d(TTAGGG)]_4$ in the presence of 0.5 equiv of heme(Fe^{3+}) in 300 mM KCl and 50 mM potassium phosphate buffer at pH 9.80 and 25 °C. The spectral regions 300−700 nm (left) and 450−700 nm (right) are shown.

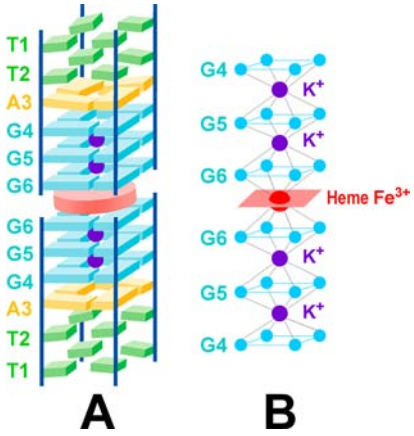

Figure 7. Schematic representation of (A) structure of the heme(F^{3+})−DNA complex determined in this study and (B) interaction of the heme Fe^{3+} (red circle) and K^+ ions (purple circles) with the guanine carbonyl oxygen atoms of the G-quartets. The heme(Fe^{3+}) is sandwiched between the 3′-terminal G-quartets of the G-quadruplex DNA formed from d(TTAGGG), and the heme Fe^{3+} interacts with the eight oxygen atoms of two G6 G-quartets.

conditions used in the study. The observed intermolecular NOE results (Figure 3), together with the 1:2 complexation between the heme(Fe^{3+}) and G-quadruplex DNA, as revealed by both analysis of the NMR signal intensities and the optical study (see Figures S9 and S10 in the Supporting Information), demonstrated that heme(Fe^{3+}) is sandwiched between the G6 G-quartets, as illustrated in Figure 7. The stacking of the pseudo-C_2-symmetric heme onto the C_4-symmetric G-quartet should result in the formation of heme orientational isomers, as has been demonstrated previously.[14] Heme orientational isomers, however, are thought to be completely absent for the heme sandwiched between the G-quartets. Therefore, the absence of heme orientational isomers in the present complex, as revealed by the NMR results, is consistent with the structure in Figure 7. Furthermore, the low-spin heme(Fe^{3+}) sandwiched between the G-quadruplex DNAs was also consistent with the MCD and CD results, which suggested the coordination of rather strong field ligands to the heme Fe^{3+} in the complex and that heme(Fe^{3+}) is surrounded by the right-handed helical environment of the DNAs, respectively. Additionally, the increased thermostability of the G-quadruplex DNA upon heme(Fe^{3+}) binding (Figure 4) could be reasonably explained on the basis of the determined structure.

Heme Electronic Structure in the Heme(Fe^{3+})−DNA Complex. The heme side-chain methyl proton signals observed at 9−15 ppm were characteristic of a heme(Fe^{3+}) LS species.[47] In addition, the heme methyl proton shift pattern of 2-Me < 7-Me < 18-Me < 12-Me, in order of increasing downfield shift, and the value of 4.44 ppm for the spread of the heme methyl proton signals at 25 °C (Table 2) were similar to the corresponding data for the bis-cyano complex of heme-(Fe^{3+}):[48] 2-Me < 7-Me < 12-Me <18-Me and 4.70 ppm, respectively. The remarkably small spread of the heme methyl proton signals of the heme(Fe^{3+})−DNA complex indicated that the in-plane asymmetry of its heme electronic structure is quite low. Since the spin state of heme Fe and the symmetry of the heme electronic structure are closely related to the nature of the bonding between the heme Fe and axial ligands,[38] the formation of a heme(Fe^{3+}) LS species, with a highly symmetric heme electronic structure, in the complex suggested that axially symmetric ligands possessing a rather strong ligand field are coordinated to heme Fe^{3+} as axial ligands. Consequently, the

dx.doi.org/10.1021/ic3005739 | Inorg. Chem. 2012, 51, 8168−8176

coordination of OH^- to the heme Fe^{3+} in the complex is thought to be quite unlikely.

Interaction between Heme(Fe^{3+}) and DNA in the Complex. The dimer of G-quadruplex DNA formed from d(TTAGGG) possesses a six-G-quartet stack, with a linear array of at least five K^+ between the G-quartets.[49,50] The K^+ ions between the G-quartets interacts electrostatically with the carbonyl oxygen atoms of the nearby eight guanine bases to stabilize the G-quartet structure through reduction of the possible electrostatic repulsion among the electrons of these oxygen atoms. Since heme(Fe^{3+}) possesses a net +1 charge, it can act as a cation like K^+ to stabilize the G-quartet structure. Consequently, although K^+ ions between the G6 G-quartets in the dimer are thought to be replaced by heme(Fe^{3+}) upon the formation of the heme(Fe^{3+})−DNA complex, the electrostatic repulsion among the oxygen atoms of the G6 G-quartets could be in part decreased by the positive charge of heme(Fe^{3+}). Thus, the binding of the heme(Fe^{3+}) between the G6 G-quartets in the DNA dimer can be stabilized through electrostatic interactions as well as the $\pi-\pi$ stacking interaction between the porphyrin moiety of the heme and the G-quartets. Consequently, judging from the stability of the complex, the possibility of OH^- coordination to heme Fe^{3+} can also be precluded, because neutralization of the net +1 charge of heme(Fe^{3+}) by the coordinated OH^- could result in a sizable loss of stabilization energy of the complex.

An interaction between the heme(Fe^{3+}) and G6 G-quartets in the complex was clearly manifested in the solvent $^1H/^2H$ isotope effects observed on the shifts and line widths of the paramagnetically shifted heme methyl proton signals of the complex (Figure 5). The heme electronic structures of paramagnetic hemoproteins have been shown to be subject to a solvent $^1H/^2H$ isotope effect.[51−54] The heme electronic structures in the proteins are perturbed by the electronic nature of Fe^{3+}-bound ligands, which has been shown to be affected by the solvent $^1H/^2H$ isotope composition through the effect of the $^1H/^2H$ replacement on the hydrogen bond between the Fe^{3+}-bound ligand and its bond partner.[51,52] Consequently, the solvent $^1H_2O/^2H_2O$ composition perturbs the heme electronic structure through its effect on the electronic nature of the Fe-bound ligand, and hence such an effect is manifested in the NMR parameters of all heme proton signals. Furthermore, since a heme proton signal exhibiting a large paramagnetic shift is in general more highly sensitive to the heme electronic structure, the magnitude of the solvent $^1H/^2H$ isotope effect on a heme proton signal is expected to depend upon its paramagnetic shift. In fact, the shifts of all four heme methyl proton signals of the heme(Fe^{3+})−DNA complex were affected by the $^1H_2O/^2H_2O$ composition, and the shift changes due to the solvent $^1H/^2H$ isotope effect correlated well with their paramagnetic shifts (Figure 5). These results indicated that the heme electronic structure in the complex is perturbed by the $^1H_2O/^2H_2O$ composition-dependent electronic nature of the Fe^{3+}-bound ligand. As described above, a G-quartet itself can be considered as a potential candidate for a Fe^{3+}-bound ligand in the heme(Fe^{3+})−DNA complex. With the structure of the complex in Figure 7, the electrons of the carbonyl oxygen atoms of G6 G-quartets can interact with the positive charge of heme Fe^{3+}. Since the carbonyl oxygen atoms of a G-quartet participate in the hydrogen-bond networks of Hoogsteen-type base pairings (see inset of Figure 1), their electronic nature is likely to be altered by the effect of the $^1H/^2H$ replacement on the hydrogen-bond networks.

The heme Fe^{3+} in the present complex can interact with each of the eight carbonyl oxygen atoms of the G6 G-quartets. Simultaneous interaction of the heme Fe^{3+} with all the oxygen atoms possibly provides a strong and axially symmetric ligand field surrounding the heme Fe^{3+}, although the field due to each $Fe^{3+}-O$ interaction may not be necessarily strong. Furthermore, the solvent $^1H/^2H$ isotope effect observed on the line widths of the heme methyl proton signals of the complex could also be attributed to the effect of the $^1H/^2H$ replacement on the hydrogen-bond networks of G-quartets. Since the heme methyl proton shift of the complex is affected by the effect of the $^1H/^2H$ replacement on the hydrogen-bond networks of the G6 G-quartets, the number of observed signals for a given heme methyl proton and the deviation in shifts and intensities of the signals are determined by the probability distribution of the $^1H/^2H$ replacement of the Hoogsteen-type base pairings associated with each G6 G-quartet. This could explain the largest line width of the heme methyl proton signals of the complex observed with ^2H_2O contents of ∼50%. Thus, the broadening of the heme methyl proton signals of the complex with the ^2H_2O contents of ∼50% is due not to exchange broadening but to overlapping of several signals exhibiting slightly different shifts from each other.

The coordination of the carbonyl oxygen atoms of a G-quartet to the heme Fe^{3+} is a salient characteristic of the present heme−DNA complex. Interaction between G-quadruplex DNA and various metal−salen (or salphen) complexes has been investigated extensively by Vilar and Neidle and co-workers.[55−58] According to the X-ray structures of complexes between the DNA and $Ni^{2+}-$ (or $Cu^{2+}-$) salphen complexes,[58] binding of the metal complexes to DNA has been shown to be stabilized primarily by $\pi-\pi$ stacking interactions between the salphen moiety of the metal complex and the G-quartets, and hence optimization in the $\pi-\pi$ stacking interaction between them has been shown to be preferable over coordination of the G-quartet to the metal center of the complex. As a result, a coordination bond between the G-quartet and the metal center of the complex is not formed in these complexes. Thus interaction between metal complexes and G-quadruplex DNA is crucially affected by the structural and electronic nature of the metal complex.

Finally, heme−DNA complexes have been shown to exhibit catalytic activities similar to those of heme enzymes such as peroxidase and peroxygenase.[15−20] Elucidation of the molecular mechanisms responsible for such catalytic activities of the complexes is one of the central issues in the field. In accord with the mechanism of hydrogen peroxide activation in heme enzymes,[59] hydrogen peroxide is thought to be coordinated to heme Fe in an "activated form" of the heme−DNA complex. Apparently, in the heme Fe^{3+} coordination structure of the present complex, no coordination site is available for hydrogen peroxide. As described in this study and our previous ones,[9,12,14] the structure of the complex as well as the heme Fe coordination structure in the complex is highly affected by solution conditions. Further characterization of both the structure and catalytic activity of the complex is needed to elucidate its function at the atomic level.

■ CONCLUSION

We have demonstrated that heme(Fe^{3+}) is sandwiched between the 3′-terminal G-quartets of G-quadruplex DNAs formed from d(TTAGGG) under the solution conditions used in this study.

dx.doi.org/10.1021/ic3005739 | Inorg. Chem. 2012, 51, 8168−8176

In this unique complex, heme Fe^{3+} interacts with the eight carbonyl oxygen atoms of two G-quartets, and such an interaction provides a strong and axially symmetric ligand field surrounding the heme Fe^{3+}, yielding a heme(Fe^{3+}) LS species with a highly symmetric heme electronic structure. This finding provides new insights as to the design of the molecular architecture and functional properties of various heme(Fe^{3+})−DNA complexes.

■ ASSOCIATED CONTENT

Supporting Information

One table and 14 figures showing ^{1}H NMR signal assignments for G-quadruplex DNA, d[TTAGGG]$_4$; schematic representation of intermolecular NOEs observed between heme(Fe^{3+}) and [d(TTAGGG)]$_4$ in the heme(Fe^{3+})−[d(TTAGGG)]$_4$ complex; portions of NOESY and NOE difference spectra of the heme(Fe^{3+})−[d(TTAGGG)]$_4$ complex; recovery of guanine imino and heme 2-Me proton signals of [d(TTAGGG)]$_4$ and the heme(Fe^{3+})−[d(TTAGGG)]$_4$ complex; ^{1}H NMR spectrum of d[TTAGGG]$_4$ in the presence of ∼0.3 equiv of heme(Fe^{3+}); UV−vis absorption spectra, 305−495 nm, of 4.0 μM heme(Fe^{3+}) in the presence of various concentrations of [d(TTAGGG)]$_4$; Scatchard plots of 406-nm absorption; and MCD, CD, and absorption spectra of the heme(Fe^{3+})−[d(TTAGGG)]$_4$ complex and ferric Mb. This material is available free of charge via the Internet at http://pubs.acs.org.

■ AUTHOR INFORMATION

Corresponding Author

*(Y.Y.) Phone/fax: +81 29 853 6521, e-mail: yamamoto@chem.tsukuba.ac.jp. (N.K.) Phone/fax: +81 22 795 7719, e-mail: nagaok@m.tohoku.ac.jp.

Notes

The authors declare no competing financial interest.

■ ACKNOWLEDGMENTS

This work was supported by Grants-in-Aid for Scientific Research on Innovative Areas (23108703 and 20108007, π-Space) and 23655151 from MEXT, the Yazaki Memorial Foundation for Science and Technology, and the Novartis Foundation (Japan) for the Promotion of Science

■ REFERENCES

(1) Sen, D.; Gilbert, W. *Nature* **1988**, *334*, 364−366.
(2) Sen, D.; Gilbert, W. *Biochemistry* **1992**, *31*, 65−70.
(3) Laughlan, G.; Murchie, A. I. H.; Norman, D. G.; Moore, M. H.; Moody, P. C. E.; Liley, D. M. J.; Luisi, B. *Science* **1994**, *265*, 520−524.
(4) Parkinson, G. N.; Lee, M. P. H.; Neidle, S. *Nature* **2002**, *417*, 876−880.
(5) Hurley, L. H.; Wheelhouse, R. T.; Sun, D.; Kerwin, S. M.; Salazar, M.; Fedoroff, O. Y.; Han, F. X.; Han, H.; Izbicka, E.; Von Hoff, D. D. *Pharmacol. Ther.* **2000**, *85*, 141−158.
(6) Han, H.; Hurley, L. H. *Trends Pharmacol. Sci.* **2000**, *21*, 136−142.
(7) Shi, D. F.; Wheelhouse, R. T.; Sun, D.; Hurley, L. H. *J. Med. Chem.* **2001**, *44*, 4509−4523.
(8) Han, H.; Langley, D. R.; Rangan, A.; Hurley, L. H. *J. Am. Chem. Soc.* **2001**, *123*, 8902−8913.
(9) Mikuma, T.; Ohyama, T.; Terui, N.; Yamamoto, Y.; Hori, H. *Chem. Commun.* **2003**, 1708−1709.
(10) Ohyama, T.; Kato, Y.; Mita, H.; Nagatamo, S.; Yamamoto, Y. *Nucleic Acid Symp. Ser.* **2005**, *49*, 245−246.
(11) Mita, H.; Ohyama, T.; Tanaka, Y.; Yamamoto, Y. *Biochemistry* **2006**, *45*, 6765−6772.
(12) Ohyama, T.; Kato, Y.; Mita, H.; Yamamoto, Y. *Chem. Lett.* **2006**, *35*, 126−127.
(13) Saito, K.; Nakano, Y.; Tai, H.; Nagatamo, S.; Hemmi, H.; Mita, H.; Yamamoto, Y. *Nucleic Acid Symp. Ser.* **2009**, *53*, 241−242.
(14) Saito, K.; Tai, H.; Fukaya, M.; Shibata, T.; Nishimura, R.; Neya, S.; Yamamoto, Y. *J. Biol. Inorg. Chem.* **2012**, *17*, 437−445.
(15) Tavascio, P.; Li, Y.; Sen, D. *Chem. Biol.* **1998**, *5*, 505−517.
(16) Tavascio, P.; Witting, P. K.; Mauk, A. G.; Sen, D. *J. Am. Chem. Soc.* **2001**, *123*, 1337−1348.
(17) Tavascio, P.; Witting, P. D.; Mauk, A. G.; Sen, D. *Inorg. Chem.* **2001**, *40*, 5017−5023.
(18) Poon, L. C.; Methot, S. P.; Morabi-Pazooki, W.; Pio, F.; Bennet, A. J.; Sen, D. *J. Am. Chem. Soc.* **2011**, *133*, 1877−1884.
(19) Golub, E.; Freeman, R.; Willner, I. *Angew. Chem., Int. Ed.* **2011**, *50*, 11710−11714.
(20) Stefan, L.; Denat, F.; Monchaud, D. *J. Am. Chem. Soc.* **2011**, *133*, 20405−20415.
(21) Wang, Y.; Patel, D. J. *Biochemistry* **1992**, *31*, 8112−8119.
(22) Kato, Y.; Ohyama, T.; Mita, H.; Yamamoto, Y. *J. Am. Chem. Soc.* **2005**, *127*, 9980−9981.
(23) Antonini, E.; Brunori, M. *Hemoglobins and Myoglobins in their Reactions with Ligands*; North Holland Publishing: Amsterdam, 1971; pp 43−48.
(24) Giacometti, G. M.; Da Ros, A.; Antonini, E.; Brunori, M. *Biochemistry* **1975**, *14*, 1584−1588.
(25) Iizuka, T.; Morishima, I. *Biochim. Biophys. Acta* **1975**, *400*, 143−153.
(26) McGrath, T. M.; La Mar, G. N. *Biochim. Biophys. Acta* **1978**, *534*, 99−111.
(27) Pande., U.; La Mar, G. N.; Lecomte, J. T. J.; Ascoli, F.; Brunori, M.; Smith, K. M.; Pandey, R. K.; Parish, D. W.; Thanabal, V. *Biochemistry* **1986**, *25*, 5638−5646.
(28) Nagao, S.; Hirai, Y.; Suzuki, A.; Yamamoto, Y. *J. Am. Chem. Soc.* **2005**, *127*, 4146−4147.
(29) La Mar, G. N.; Davis, N. L.; Parish, D. W.; Smith, K. M. *J. Mol. Biol.* **1983**, *168*, 887−896.
(30) La Mar, G. N.; Toi, H.; Krishnamoorthi, R. *J. Am. Chem. Soc.* **1984**, *106*, 6395−6401.
(31) La Mar, G. N.; Yamamoto, Y.; Jue, T.; Smith, K. M.; Pandey, R. K. *Biochemistry* **1985**, *24*, 3826−3831.
(32) McLachlan, S. J.; La Mar, G. N.; Burns, P. D.; Smith, K. M.; Langry, K. C. *Biochim. Biophys. Acta* **1986**, *874*, 274−284.
(33) Du, W.; Syvitski, R.; Dewilde, S.; Moens, L.; La Mar, G. N. *J. Am. Chem. Soc.* **2003**, *125*, 8080−8081.
(34) Li, T.; Dong, S.; Wang, E. *Chem.—Asian J.* **2009**, *4*, 918−922.
(35) Pitto, M.; Saudek, V.; Sklenar, V. *J. Biomol. NMR* **1992**, *2*, 661−666.
(36) Sklenar, V.; Pitto, M.; Leppik, R.; Saudek, V. *J. Magn. Reson., Ser. A* **1993**, *102*, 241−245.
(37) States, D. J.; Haeberkorn, R. A.; Ruben, D. J. *J. Magn. Reson.* **1982**, *72*, 286−292.
(38) Yamamoto, Y. *Annu. Rep. NMR Spectrosc.* **1998**, *36*, 1−77.
(39) Smith, D. W.; Williams, R. J. P. *Struct. Bonding (Berlin)* **1970**, *7*, 1−45.
(40) Kobayashi, N. *Inorg. Chem.* **1985**, *24*, 3324−3330.
(41) Matsuoka, A.; Kobayashi, N.; Shikama, K. *Eur. J. Biochem.* **1992**, *210*, 337−341.
(42) Ikeda-Saito, M.; Hori, H.; Anderson, L. A.; Prince, R. C.; Pickering, I. J.; George, G. N.; Sanders, C. R.; Luts, R. S.; McKelvey, E. J.; Matera, R. *J. Biol. Chem.* **1992**, *267*, 22843−22852.
(43) Nozawa, T.; Kobayashi, N.; Hatano, M. *Biochim. Biophys. Acta* **1976**, *427*, 652−662.
(44) Vickery, L.; Nozawa, T.; Sauer, K. *J. Am. Chem. Soc.* **1976**, *98*, 343−350.
(45) Kobayashi, N.; Higashi, R.; Titeca, T. C.; Lamote, F.; Ceulemans, A. *J. Am. Chem. Soc.* **1999**, *121*, 12018−12028.
(46) Kobayashi, N.; Muranaka, A.; Mack, J. *Circular Dichroism and Magnetic Circular Dichroism Spectroscopy for Organic Chemists*; Royal Society of Chemistry: London, 2011.

(47) La Mar, G. N. In *Biological Applications of Magnetic Resonance*; Shulman, R. G., Ed.; Academic Press: New York, 1979; pp 305−343.
(48) Yamamoto, Y.; Fujii, N. *Chem. Lett.* **1987**, 1073−1076.
(49) Haider, S.; Parkinson, G. N.; Neidle, S. *J. Mol. Biol.* **2002**, *320*, 189−200.
(50) Hazel, P.; Parkinson, G. N.; Neidle, S. *J. Am. Chem. Soc.* **2006**, *128*, 5480−5487.
(51) Lecomte, J. T. J.; La Mar, G. N. *J. Am. Chem. Soc.* **1987**, *109*, 7219−7220.
(52) La Mar, G. N.; Chatfield, M. J.; Peyton, D. H.; de Ropp, J. S.; Smith, W. S.; Krishnamoorthi, R.; Datterlee, J. D.; Erman, J. E. *Biochim. Biophys. Acta* **1988**, *956*, 267−276.
(53) Yamamoto, Y.; Iwafune, K.; Chujo, R.; Inoue, Y.; Imai, K.; Suzuki, T. *J. Mol. Biol.* **1992**, *228*, 343−346.
(54) Tai, H.; Nagatomo, S.; Mita, H.; Sambongi, Y.; Yamamoto, Y. *Bull. Chem. Soc. Jpn.* **2005**, *78*, 2019−2025.
(55) Reed, J. E.; Arola-Arnal, A.; Neidle, S.; Vilar, R. *J. Am. Chem. Soc.* **2006**, *128*, 5992−5993.
(56) Reed, J. E.; Neidle, S.; Vilar, R. *Chem. Commun.* **2007**, 4366−4368.
(57) Arola-Arnal, A.; Benet-Buchholz, J.; Neidle, S.; Vilar, R. *Inorg. Chem.* **2008**, *47*, 11910−11919.
(58) Campbell, N. H.; Abd Karim, N. H.; Parkinson, G. N.; Gunaratnam, M.; Petrucci, V.; Todd, A. K.; Vilar, R.; Neidle, S. *J. Med. Chem.* **2012**, *55*, 209−222.
(59) Kato, S.; Ueno, T.; Fukuzumi, S.; Watanabe, Y. *J. Biol. Chem.* **2004**, *50*, 52376−52381.